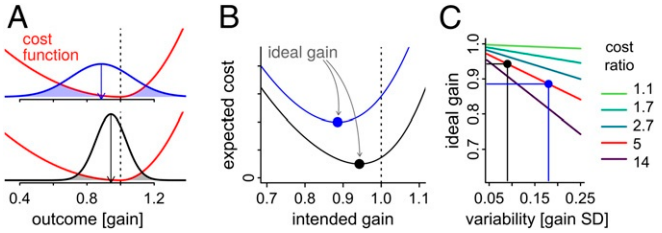

Fig. 1. Predicted relationship between saccadic variability and undershoot. (*A*) The red curve represents the cost of a saccadic error plotted against gain (proportion of target distance). The 2 Gaussian curves represent the expected distributions of motor outcomes for 2 conditions with different uncertainties about the location of the target: In the condition with larger uncertainty (blue) there is a broader range of motor outcomes for a given motor command (intended gain, represented by the vertical arrow). The expected cost for a certain intended gain is computed by integrating all possible motor outcomes, weighted by their probabilities. (*B*) The expected cost is plotted as a function of the intended gain. When uncertainty is larger, the expected cost is overall higher, and the ideal gain (which minimizes the expected cost) shifts toward more hypometric values. (*C*) Relationship between ideal gain and saccadic endpoint variability, for different degrees of asymmetry. The asymmetry is quantified as the ratio between the cost of an overshoot relative to that of an undershoot of the same size. Since the asymmetry determines the slope of the relationship between gain and variability, it is possible to estimate it by measuring (at least) 2 different conditions with varying levels of uncertainty.

range effect would appear as uncertainty increased. Indeed, any central tendency bias (13) arising from a probabilistic combination of sensory likelihood and prior knowledge should increase as the likelihood becomes more diffuse.

Results

To test the 2 predictions mentioned in the Introduction, we conducted a series of experiments in which we manipulated the positional uncertainty of the saccadic target, as well as the range of its possible positions (thus their prior probabilities), and measured how these factors contribute to constant and variable saccadic errors. We were interested in simple visual orienting responses; therefore we avoided adding more explicit tasks that may have influenced the cost function. We expected both the hypometric bias and the range effect to increase with increasing uncertainty. In experiment 1 ($n = 12$) we manipulated the uncertainty by blurring a Gaussian blob embedded in noise (keeping the total luminance energy constant; Fig. 2*A*) and measured saccadic responses in 2 sessions, run on separate days, that contained different ranges of target eccentricities (this was necessary to measure the range effect). Although positional uncertainty should be reflected in the distribution of saccade endpoints, to make sure that our manipulation was successful, we also measured each observer's perceptual precision for comparing the eccentricities of blurred targets in a purely psychophysical task. The results confirmed that blurring the targets increases the uncertainty of judgments about their positions (*SI Appendix*). To characterize further the relationship between sensory uncertainty and saccadic targeting, we conducted 2 additional experiments. In experiment 2 ($n = 20$), we varied independently the size and the peak luminance of the saccadic target (Fig. 2*A*). This experiment determined the relative contributions of pure changes in target size and visibility. In experiment 3 ($n = 26$), we further investigated the robustness of the saccadic range effect by running the 2 sessions in the same day and using targets that varied only in visibility (but not size). Since these experiments provide complementary findings, in the following we report the results organized by thematic points. Detailed information about experimental procedures and statistical modeling is reported in *SI Appendix*.

Positional Uncertainty Increases Saccadic Variability and Hypometria. We found that increasing the space constant of a Gaussian blob increased the variability of the amplitudes of saccades directed to it, $F(2, 22) = 5.66$, $P = 0.01$. Crucially, we found that greater uncertainty increased not only the variable error, but also the undershoot (Fig. 2*B*). We assessed the variations of saccadic undershoot by means of a multilevel (mixed-effects) linear model (see *SI Appendix* for details), with saccadic amplitude as the dependent variable and target distance and blob's σ as predictors. The estimates of model parameters indicate that the saccadic gain (the slope of the linear relationship between saccadic amplitudes and target distance) was already hypometric in the condition with smallest σ (baseline gain 0.93 ± 0.06, mean $\pm$ SE) and became even more hypometric as σ increased: The differences from baseline were -0.01 ± 0.03, for the condition with $\sigma = 0.9°$, and -0.17 ± 0.03, for the condition with $\sigma = 1.5°$. The finding of a simultaneous increase in variable and constant errors is to be expected under the hypothesis of an asymmetrical cost function (Fig. 1). Moreover, the total changes in variability and bias (quantified as the difference between the conditions with largest and smallest uncertainty) were correlated across participants (Pearson's $r = -0.73$, 95% CI [-0.92, -0.23]): Participants who showed the largest increase in endpoint variability also displayed the largest decrease in saccadic gain, suggesting a systematic relationship between variability and bias.

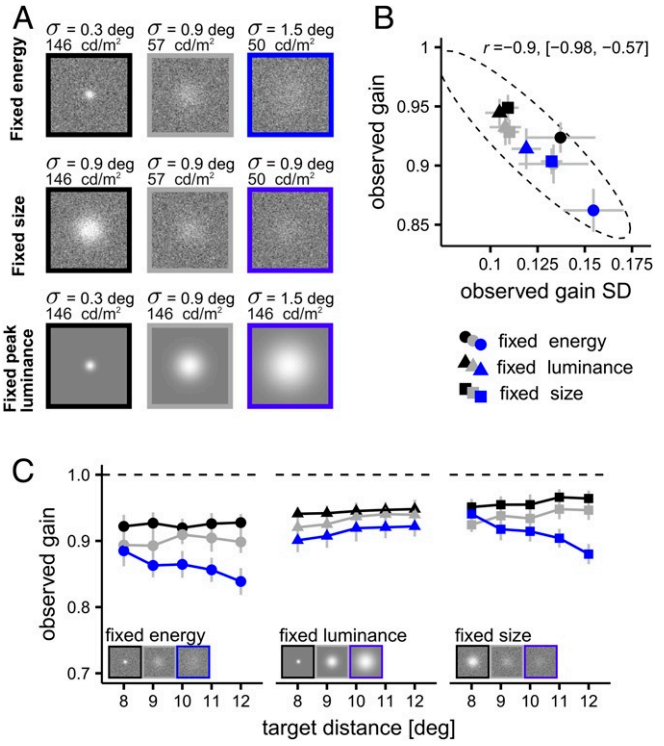

Fig. 2. Manipulation of positional uncertainty increases both behavioral variability and saccadic undershoot. (*A*) Example of the stimuli used (see main text and *SI Appendix* for details). (*B*) Empirical relationship between variability and gain; each symbol represents the weighted average values (i.e., across observers) for the mean and SD of saccadic gain in 1 experimental condition. Saccadic gain is negatively correlated with saccadic variability, as predicted by the theory (Fig. 1). (*C*) Saccadic gain, plotted as a function of target distance (experiments 1 and 2), for 3 different manipulations of the saccadic target. Only when the luminance is varied (fixed-energy and fixed-size conditions) does the decrease in amplitude vary as a function of target distance, suggesting the presence of a central bias. All error bars are bootstrapped SEs.

The blur manipulation used in experiment 1 simultaneously decreased the target's peak luminance and increased its size. Saccades might have been biased toward the nearest edge of the target [e.g., the nearest zero-crossing in the second derivative or perhaps the half-height of the luminance profile (14)]. The relative contributions of visibility and size could not have been distinguished within experiment 1, so we designed experiment 2 to discriminate between them. The procedure was similar; however, we varied the stimuli in 2 distinct conditions. In the first condition size (σ) was kept constant, while we varied the peak luminance (fixed size; Fig. 2*A*); this condition was designed to measure how visibility and signal-to-noise ratio affect saccadic eye movements when size is kept constant. In the second condition we kept luminance fixed at its maximum value, removed the background noise (minimizing the possible sources of uncertainty), and varied the size (σ) of the blobs (fixed luminance); this condition was designed to isolate modulations of saccadic movements that were due only to variations of target size.

We found that both manipulations increased the variability of saccadic gain: Fixed luminance, $F(2, 38) = 11.29$, $P = 1.42 \times 10^{-4}$; and fixed size, $F(2, 38) = 16.84$, $P = 5.8 \times 10^{-6}$. Variability, however, increased up to higher levels in the fixed-size than in the fixed-luminance condition, $t(19) = 3.51$, $P = 0.002$. In both conditions, the increase in variability was accompanied by a decrease in saccadic amplitudes, albeit with some qualitatively different features. To quantify these features, we fitted the data from each condition with a multilevel (mixed-effects) linear model, which had saccadic amplitude as a dependent variable and target distance and uncertainty level (indexed either by the blob's σ or by its peak luminance) as predictors. In the fixed-luminance condition, the decrease in amplitude was constant with respect to the distance of the target, so that the slope of the linear relationship between saccadic amplitude and target distance did not vary systematically with the value of σ, $\chi^2(2) = 0.66$, $P = 0.72$. Analysis of the fixed-size condition instead revealed a different pattern. We found that, relative to the baseline where the peak luminance was 146 cd/m^2, the decrease in saccadic amplitude was not uniform across target distances, as indicated by a significant interaction between distance and luminance, $\chi^2(2) = 30.06$, $P = 2.96 \times 10^{-7}$. This result indicates that the decrease in saccadic gain was modulated by the eccentricity of the target: Gain decreased more when eccentricity was larger (Fig. 2*C*). This finding suggests a bias toward intermediate eccentricities contingent on the visibility of the target, corresponding to the range effect mentioned in the Introduction (9, 10) (next section).

Saccadic Range Effect Depends on Positional Uncertainty. In experiments 1 and 3, each participant was tested under 2 different conditions, with different ranges of target eccentricity (Fig. 3). Here we analyzed the effect of the eccentricity range ("large" vs. "small" eccentricity range) on saccadic behavior. We started by examining how saccades made toward the intermediate targets (present in both ranges) were influenced by the session. In agreement with recent reports (11, 12), we found no evidence for a central tendency bias when uncertainty was smallest (σ = 0.3 or luminance 146 cd/m^2), as indicated by the absence of systematic differences between saccadic amplitudes directed toward the intermediate targets (experiment [Exp.] 1, $t(11) = 0.59$, $P = 0.57$; Exp. 3, $t(11) = 0.37$, $P = 0.71$). However, analogous differences varied systematically across conditions with different uncertainties, as indicated by a significant interaction between range and uncertainty level: Exp. 1, $F(1, 23) = 15.05$, $P = 7.59 \times 10^{-4}$; Exp. 3, $F(1, 23) = 15.05$, $P = 0.01$ (2-way repeated-measures ANOVA).

To quantify more precisely the range effect using all saccades (and not only those directed at the intermediate target) we assumed that the effect was due to a compression of saccadic

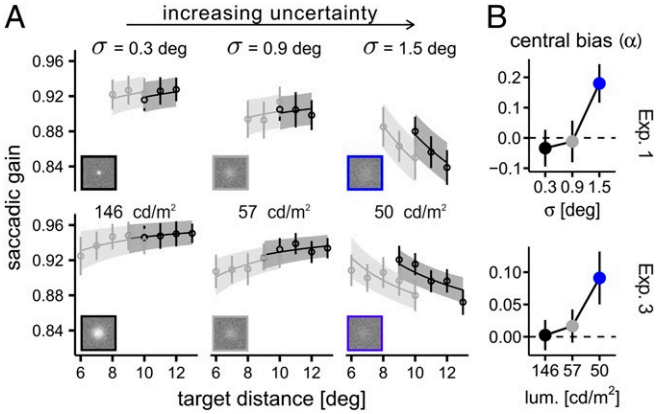

Fig. 3. The range effect. (*A*) Mean saccadic gain measured in experiments 1 and 3, plotted as a function of target distance, and split according to the eccentricity range of the experimental session. Circles indicate the average gain, while the lines are the predictions of the multilevel model fit to the data. For the 2 conditions with smaller uncertainties (leftmost subpanels), average saccadic gains toward the intermediate targets (present in both "large" and "small" sessions) are overlapping, indicating that saccades were not systematically influenced by the eccentricity range of the targets. Only in the condition with the largest uncertainty (rightmost panel) did we find an effect of eccentricity range (i.e., a central bias). (*B*) Size of the central bias, quantified as the parameter α of the regression model (*Results*) and plotted as a function of the space constant (experiment 1) or the peak luminance (experiment 3) of the target. All error bars and bands are SEs.

responses toward the mean of target eccentricity in the block (a form for central tendency bias) and estimated the amount of compression using a linear regression approach. The regression model can be expressed as $\hat{S}_i = \beta_0 + \beta_1[\alpha\bar{E} + (1-\alpha)E_i]$, where $\hat{S}_i$ and E_i are the predicted saccadic amplitude and the target eccentricity at trial i, $\bar{E}$ is the average eccentricity in the current session, and α is a weighting parameter. Positive values of α indicate a bias toward the mean eccentricity, quantified as the proportion of compression, such that a value of $\alpha = 1$ would indicate that all saccades targeted the same central location, regardless of the trial-by-trial target eccentricities. All parameters were allowed to vary across conditions with different σ. We estimated a Bayesian mixed-effects version of this model, with participant as a grouping factor (see *SI Appendix* for details). We calculated 95% credible intervals for the fixed-effect estimates of the weighting parameter α and found that the amount of compression differed significantly from 0 only in the condition with largest uncertainty: Experiment 1, $\sigma = 1.5$, $\alpha = 0.18$, 95% CI [0.06, 0.30]; experiment 3, peak luminance 50 cd/m^2, $\alpha = 0.09$, 95% CI [0.01, 0.17] (Fig. 3*B*). Thus, our results indicate that although a range effect is not normally present for small, highly visible targets, a systematic bias toward the mean eccentricity nonetheless emerges when uncertainty increases.

Cost Asymmetry Determines the Relationship between Saccadic Variability and Bias. We suggest that the observed modulations of saccadic gain are a consequence of the oculomotor system seeking to minimize a cost function, in which overshoots and undershoots are given different weights. If an asymmetrical cost function were underlying the relationship between saccadic variability and undershoot, then it should be possible to estimate the degree of asymmetry, as shown in Fig. 1. To simplify the analysis, we transformed saccadic amplitudes in gain values (proportions of target distance) and pooled data from different target eccentricities together. This allowed us to specify a unique cost function for all eccentricities, where the error is defined in gain units. We assumed that cost would be well approximated by a quadratic function of the error, augmented with

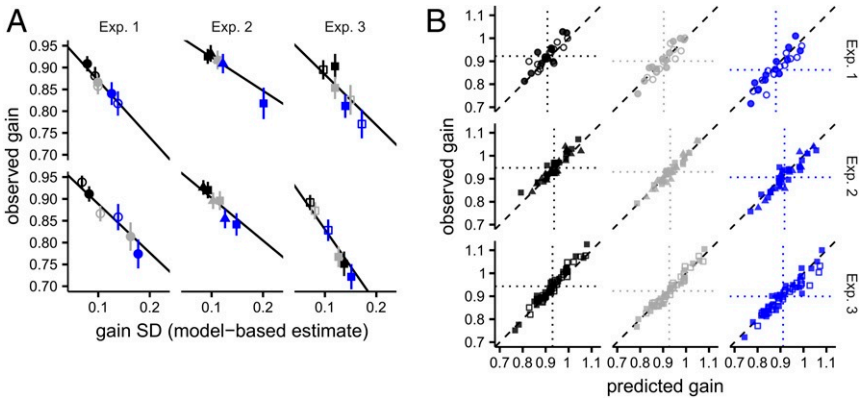

Fig. 4. Cost asymmetry determines the relationship between saccadic variability and bias. (*A*) Estimated relationship between saccadic variability and bias for some example participants (2 participants for each of the 3 experiments). The average saccadic gain for each condition and session is plotted as a function of the variability, as estimated by the model. Black lines represent the predicted gain, assuming the optimization of an asymmetrical, quadratic cost function. (Symbols follow the same conventions as in Fig. 2, with one additional feature: for the experiments divided into sessions with different eccentricity ranges, solid and open symbols indicate small and large sessions, respectively.). Error bars are 95% CIs. (*B*) Predicted and observed saccadic gain for all of the participants, split by condition and experiment. The vertical and horizontal dotted lines indicate group means. See *SI Appendix*, Fig. S1 for a similar plot showing observed and predicted SDs of saccadic gain.

an additional asymmetry term that set a fixed ratio between the cost of undershoot and overshoot errors (see *SI Appendix* for details). Maximum-likelihood estimates of the asymmetry parameter indicate that participants behaved as if they were optimizing an asymmetrical cost function where overshoot errors were considered about 7.5 times costlier (median across participants) than undershoots in experiment 1, 95% CI [3.0, 15.7]; 6.7 times costlier in experiment 2, 95% CI [2.9, 8.5]; and 7.7 times costlier in experiment 3, 95% CI [4.5, 18.4]. There was no significant difference in the estimated cost asymmetry across experiments, $F(2, 56) = 0.67$, $P = 0.51$. Overall, the assumption of an asymmetric, quadratic cost function provides a good fit to variations in saccadic gain across all our experiments (Fig. 4). We used a leave-one-out cross-validation procedure to evaluate the predictive ability of the quadratic-asymmetric model against a descriptive model, which assumed only that the undershoot bias has a linear relationship with saccadic variability, without requiring that this relationship be adequate for minimizing an asymmetrical cost function. Across the 3 experiments, this test confirmed that assuming an asymmetric cost function results in a better and more parsimonious description of the data (*SI Appendix*).

As an additional test of our hypothesis, we investigated whether gain variability could account for differences in gain, after controlling for the effects of our manipulations. For each experiment, we fitted a multilevel linear model with the saccadic gain as the dependent variable, luminance or space constant as the categorical predictor, and participant as the grouping factor. We took the residuals of these models and computed the correlation to the SD of saccadic gain. We found a significant correlation (Pearson's $r = -0.14$, 95% CI [−0.26, −0.11]), which indicates that even after controlling for the influence of our manipulation, saccadic variability retains information about saccadic gain, a remarkable result given the individual differences in the degree of asymmetry of the cost function (next section).

Cost Asymmetry Is Related to the Programming of Corrective Saccades. We examined further whether individual differences in the asymmetry of the cost function could be related to differences in the postsaccadic processing of the target. Across our 3 experiments we recorded a large number of secondary saccades (see *SI Appendix* for details), which can be appropriately defined as corrective because their amplitude was negatively correlated with residual error of the primary saccade (Fig. 5*A*). As mentioned in the Introduction, corrective saccades tend to have longer latencies when they are made in the direction opposite to that of the primary saccade (5–7), suggesting that overshoots and undershoots have different consequences for postsaccadic oculomotor processing. The latencies of small saccades, however, are also modulated by their amplitudes, which are often larger after undershoot errors (because they are larger, on average, than overshoots). To control for this effect, before segregating forward and backward corrective saccades (that is, in the opposite and the same direction as the primary one, respectively), we fitted a quadratic model to the latency of secondary saccades (as the dependent variable) as a function of their amplitudes (*SI Appendix* and Fig. 5). We took the residuals of this model and classified them into forward and return saccades depending on the direction relative to the primary saccade. We then took, for each participant, the difference between the mean residuals of return saccades (which were expected to have longer latencies) and those of forward saccades. This difference represents an estimate of the additional time cost required to prepare corrective saccades in the direction opposite to the primary one (Fig. 5*B*). Overall, this additional time cost was estimated to be about 30 ms, 95% CI [18, 44].

If the cost-function asymmetry that we estimated from the bias–variability relationship of primary saccades were related to this latency cost, then we should find a positive correlation between these 2 measures. Our data support this conjecture, providing clear evidence for a positive relationship (Fig. 5), Pearson's $r = 0.50$, 95% CI [0.28, 0.68]*. Computed separately for each experiment, the correlation estimates were as follows: Experiment 1, $r = 0.60$, 95% CI [0.04, 0.89]; experiment 2, $r = 0.62$, 95% CI [0.25, 0.84]; experiment 3, $r = 0.46$, 95% CI [0.07, 0.73]. To summarize, the joint analysis of secondary saccade latencies and primary saccade bias and variability indicates that the slower a participant is in correcting an overshoot error (relative to an undershoot), the more hypometric her/his saccades become with uncertainty about target location. This finding supports the notion that undershoots result from the

*To estimate the correlation we removed 3 data points (of 59) corresponding to participants for which the SE of the latency cost was larger than 30 ms (their mean SE was ≈65 ms, whereas it was only ≈18 ms for the remaining participants). Adding these less reliable data points does not change the conclusions and yields a correlation of $r = 0.41$, 95% CI [0.18, 0.60].

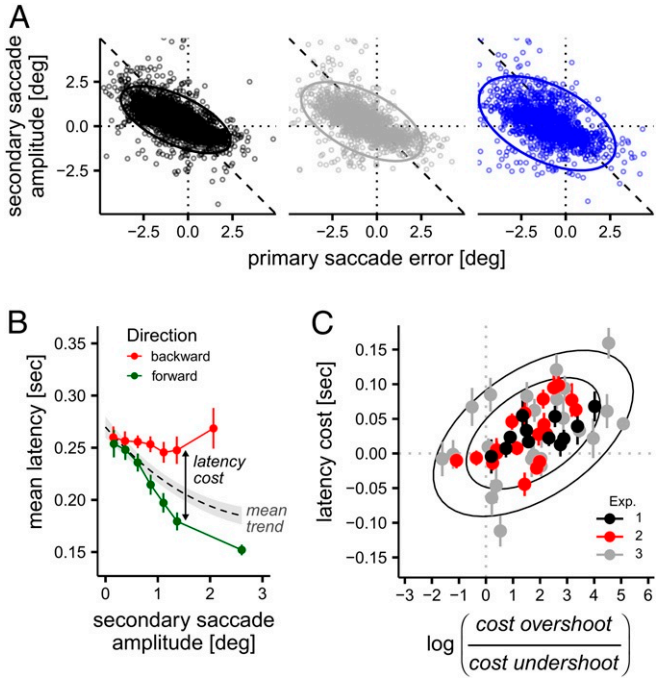

Fig. 5. Cost asymmetry is related to the programming of corrective saccades. (*A*) Secondary saccades recorded in our experiments were corrective, as indicated by their negative correlation with the error of primary saccades. (Ellipses are 95% bivariate CIs of the mean.) (*B*) The latency cost is defined as the difference in latency between backward and forward saccades, after correcting for the mean trend due to the amplitude of secondary saccades (see *SI Appendix* for details and *SI Appendix*, Fig. S2 for a plot of saccadic latencies distributions). (*C*) The relationship between estimated cost asymmetry (expressed as log-ratio of costs for an error of constant size) and the latency cost. See *SI Appendix*, Fig. S3 for a separate analysis of the latencies of forward and backward saccades. Ellipses represent 75% and 95% bivariate CIs.

visual system's strategy for keeping saccadic targets in the same visual hemifield (15) and extends that notion by showing that the parameters of primary saccades are optimized, taking into account the possibility that a secondary, corrective movement will be necessary.

Discussion

In the present study, we manipulated the positional uncertainty of a peripheral visual target and examined how the oculomotor system responded to increased uncertainty when planning saccades. In experiment 1, we found that increasing the blur of the target (a Gaussian blob embedded in noise) produced a larger spread of the saccadic landing positions and decreased the precision of positional judgments in a related perceptual task. Crucially, as the uncertainty increased, saccades also became more hypometric and systematically shifted toward the mean location of the target, a form of central tendency bias (13). The decrease in saccadic amplitude was well described by a simple model based on the assumption that the system is adapted to optimize an asymmetrical, quadratic cost function. In support of this assumption, we found that the estimated degree of asymmetry of the cost function was related across participants to the additional time required to plan a backward corrective saccade, made in the opposite direction to the primary one, relative to a forward one made in the same direction. In other words, the more time participants required to correct an overshoot (relative to an undershoot) with a secondary saccade, the more they decreased the mean amplitude of their primary saccades as the uncertainty in the target's position increased. These findings were corroborated by the results of experiments 2 and 3, which also revealed that the reduced visibility of the target is the main source of these effects, while increasing the size of the target produces only a moderate, eccentricity-invariant decrease in saccadic amplitudes. Overall, the results presented here provide empirical evidence for theories arguing that an asymmetrical cost function is the source of the typical saccadic undershoot (15, 16) and establish experimentally the presence of a probabilistic mechanism that takes into account sensory and motor uncertainty to adjust where saccades are directed.

There are several (not necessarily incompatible) reasons for why the saccadic system might have evolved to avoid overshoot errors. According to one hypothesis (16), the system might seek to minimize the overall saccadic flight time: Since visual sensitivity is much reduced during a saccade (17), it seems reasonable that the visual system may be adapted to maximize periods of clear view (even though the advantage would be only a few milliseconds per saccade). Yet another hypothesis was advanced by Robinson (15), who proposed that the system may seek to maintain the postsaccadic target in the same visual hemifield as the presaccadic one, to facilitate further processing. This idea has been further developed by Ohl *et al.* (6) and Ohl and Rolfs (18), who showed that secondary saccades are faster and more frequent after undershoots. These findings were interpreted in the context of a conceptual model, originally developed to explain the generation of microsaccades (19), which postulates that saccadic amplitudes are coded in a motor map endowed with short-range excitatory and long-range inhibitory connections. As a result, after each saccade the spatial distribution of neural activity would be biased toward the retinal location of the target in a way that facilitates further movements along a similar direction, while slowing down movements in the opposite direction. If this imbalance represented an implementation constraint of the eye plant, then the system should take it into account by adopting a strategy that reduces the likelihood of overshoot errors. Therefore, Ohl's conceptual model (6, 18) provides a biologically plausible implementation of the cost function in our model, which was formulated at a more abstract, computational level of description. Our results support this conjecture, by showing that individual differences in the latency cost (Fig 5*C*) are positively correlated with the estimated asymmetry of the cost function. Furthermore, additional analyses confirmed that individual differences in the latency cost were due to the difficulty in quickly planning backward corrective movements (*SI Appendix*, Fig. S3), rather than to the facilitation of forward corrections. This latter finding supports our interpretation that the functional role of saccadic hypometria is to avoid the slower corrections entailed by overshoot errors.

The present results help resolve a debate in the literature about the presence of a range effect (a central tendency bias) in saccadic targeting (9–12) by demonstrating that, although the range effect is not generally present when the target can be located with good precision, it does emerge when the positional uncertainty is large. In agreement with previous reports that "averaging" saccades, which tend to fall in between the target and a distractor, are biased toward the most probable location of the target (20) our results support the view that a Bayesian process is working to optimize saccadic eye movement by taking advantage of prior knowledge. Although previous research suggested the saccades are normally based only on the most recent sensory information available (21–23), our current results show that when uncertainty is particularly high, the saccadic system can reflect expectations developed over longer timescales, spanning multiple trials.

Finally, given that our experiment involved conditions of artificially high uncertainty that are uncommon in everyday life, one important issue in their interpretation is to what extent they generalize to more ecological conditions. While our

experimental conditions were specifically designed to allow precise measurements of saccadic bias and variability under conditions of varying uncertainty, previous studies have demonstrated that a systematic undershoot bias is present also under more ecological conditions, involving for example free viewing (24), visual search (25, 26), and free scanning of continuously present targets (27). High rates of error-correcting secondary saccades were found also under conditions designed to increase the difficulty of saccadic targeting during the scanning of stationary targets (28). In sum, the phenomena we examined in our study (saccadic undershoot and corrective saccades) are found also in a broad range of different and arguably more ecological experimental conditions, indicating that they reflect fundamental aspects of saccadic planning.

In conclusion, our results demonstrate that a flexible adaptive strategy underlies the control of saccadic amplitudes. By estimating the relationship between uncertainty about the target location, saccadic accuracy, and saccadic variability, we have shown that the typical undershoot bias of saccadic eye movements can be adequately explained as the result of strategy designed to optimize saccadic amplitudes, given sensorimotor uncertainty and an asymmetrical cost function. This strategy is probabilistic and Bayesian, in the sense that it must have at its disposal a trial-by-trial representation of uncertainty and it takes prior information into account. Together with previous reports that show how the distributions of saccadic landing positions are sensitive to rewards and task demands (29), the present results highlight the utility of eye-movement analysis as a tool to study probabilistic aspects of information processing in the brain.

Materials and Methods

See *SI Appendix* for the details of the experimental procedures and statistical analyses. All participants gave their informed consent in written form; the protocol of the study received full approval from the Research Ethics Committee of the School of Health Sciences of City, University of London. Data and code are available as an Open Science Framework repository: https://osf.io/293gc/.

ACKNOWLEDGMENTS. This work was supported by Grant RPG-2016-124 from the Leverhulme Trust (to M.J.M.).

1. R. J. van Beers, Saccadic eye movements minimize the consequences of motor noise. *PLoS One* **3**, e2070 (2008).
2. R. J. van Beers, The sources of variability in saccadic eye movements. *J. Neurosci.* **27**, 8757–8770 (2007).
3. C. M. Harris, D. M. Wolpert, Signal-dependent noise determines motor planning. *Nature* **394**, 780–784 (1998).
4. W. Becker, A. F. Fuchs, Further properties of the human saccadic system: Eye movements and correction saccades with and without visual fixation points. *Vis. Res.* **9**, 1247–1258 (1969).
5. H. Deubel, W. Wolf, G. Hauske, Corrective saccades: Effect of shifting the saccade goal. *Vis. Res.* **22**, 353–364 (1982).
6. S. Ohl, S. A. Brandt, R. Kliegl, Secondary (micro-)saccades: The influence of primary saccade end point and target eccentricity on the process of postsaccadic fixation. *Vis. Res.* **51**, 2340–2347 (2011).
7. S. Ohl, R. Kliegl, Revealing the time course of signals influencing the generation of secondary saccades using Aalen's additive hazards model. *Vis. Res.* **124**, 52–58 (2016).
8. F. Vitu, S. Casteau, H. Adeli, G. J. Zelinsky, E. Castet, The magnification factor accounts for the greater hypometria and imprecision of larger saccades: Evidence from a parametric human-behavioral study. *J. Vis.* **17**, 2 (2017).
9. Z. Kapoula, Evidence for a range effect in the saccadic system. *Vis. Res.* **25**, 1155–1157 (1985).
10. Z. Kapoula, D. A. Robinson, Saccadic undershoot is not inevitable: Saccades can be accurate. *Vis. Res.* **26**, 735–743 (1986).
11. C. Gillen, J. Weiler, M. Heath, Stimulus-driven saccades are characterized by an invariant undershooting bias: No evidence for a range effect. *Exp. Brain Res.* **230**, 165–174 (2013).
12. A. Nuthmann, F. Vitu, R. Engbert, R. Kliegl, No evidence for a saccadic range effect for visually guided and memory-guided saccades in simple saccade-targeting tasks. *PLoS One* **11**, e0162449 (2016).
13. H. L. Hollingworth, The central tendency of judgment. *J. Philos. Psychol. Sci. Methods* **7**, 461 (1910).
14. R. J. Watt, M. J. Morgan, The recognition and representation of edge blur: Evidence for spatial primitives in human vision. *Vis. Res.* **23**, 1465–1477 (1983).
15. D. A. Robinson, Models of the saccadic eye movement control system. *Kybernetik* **14**, 71–83 (1973).
16. C. M. Harris, Does saccadic undershoot minimize saccadic flight-time? A Monte-Carlo study. *Vis. Res.* **35**, 691–701 (1995).
17. E. B. Holt, Eye-movement and central anaesthesia. *Psychol. Rev.* **4**, 1–45 (1903).
18. S. Ohl, M. Rolfs, Saccadic eye movements impose a natural bottleneck on visual short-term memory. *J. Exp. Psychol.* **43**, 736–748 (2017).
19. M. Rolfs, R. Kliegl, R. Engbert, Toward a model of microsaccade generation: The case of microsaccadic inhibition. *J. Vis.* **8**, 5.1–5.23 (2008).
20. P. He, E. Kowler, The role of location probability in the programming of saccades: Implications for "center-of-gravity" tendencies. *Vis. Res.* **29**, 1165–1181 (1989).
21. M. Lisi, P. Cavanagh, Dissociation between the perceptual and saccadic localization of moving objects. *Curr. Biol.* **25**, 2535–2540 (2015).
22. D. Massendari, M. Lisi, P. Cavanagh, T. Collins, Is the efference copy of a saccade influenced by a perceptual illusion?*J. Vis.* **17**, 879 (2017).
23. M. Lisi, P. Cavanagh, Different spatial representations guide eye and hand movements. *J. Vis.* **17**, 12 (2017).
24. C. Rasche, K. R. Gegenfurtner, Visual orienting in dynamic broadband (1/f) noise sequences. *Atten. Percept. Psychophys.* **72**, 100–113 (2010).
25. E. McSorley, J. M. Findlay, Saccade target selection in visual search: Accuracy improves when more distractors are present. *J. Vis.* **3**, 20 (2003).
26. J. M. Findlay, Saccade target selection during visual search. *Vis. Res.* **37**, 617–631 (1997).
27. J. M. Findlay, V. Brown, Eye scanning of multi-element displays: I. Scanpath planning. *Vis. Res.* **46**, 179–195 (2006).
28. C. C. Wu, O. S. Kwon, E. Kowler, Fitts's Law and speed/accuracy trade-offs during sequences of saccades: Implications for strategies of saccadic planning. *Vis. Res.* **50**, 2142–2157 (2010).
29. A. C. Schutz, J. Trommershauser, K. R. Gegenfurtner, Dynamic integration of information about salience and value for saccadic eye movements. *Proc. Natl. Acad. Sci. U.S.A.* **109**, 7547–7552 (2012).